

## Theoretical aspects of WS<sub>2</sub> nanotube chemical unzipping

Cite this: *Nanoscale*, 2014, 6, 8400D. G. Kvashnin,<sup>\*ab</sup> L. Yu. Antipina,<sup>c</sup> P. B. Sorokin,<sup>acd</sup> R. Tenne<sup>e</sup> and D. Golberg<sup>f</sup>

Theoretical analysis of experimental data on unzipping multilayered WS<sub>2</sub> nanotubes by consequent intercalation of lithium atoms and 1-octanethiol molecules [C. Nethravathi, *et al.*, *ACS Nano*, 2013, 7, 7311] is presented. The radial expansion of the tube was described using continuum thin-walled cylinder approximation with parameters evaluated from *ab initio* calculations. Assuming that the attractive driving force of the 1-octanethiol molecule is its reaction with the intercalated Li<sup>+</sup> ions *ab initio* calculations of a 1-octanethiol molecule bonding with Li<sup>+</sup> were carried out. In addition, the non-chemical interactions of the 1-octanethiol dipole with an array of positive point charges representing Li<sup>+</sup> were taken into account. Comparing between the energy gain from these interactions and the elastic strain energy of the nanotube allows us to evaluate a value for the tube wall deformation after the implantation of 1-octanethiol molecules. The *ab initio* molecular dynamics simulation confirmed our estimates and demonstrated that a strained WS<sub>2</sub> nanotube, with a decent concentration of 1-octanethiol molecules, should indeed be unzipped into the WS<sub>2</sub> nanoribbon.

Received 22nd January 2014

Accepted 25th April 2014

DOI: 10.1039/c4nr00437j

www.rsc.org/nanoscale

The establishment of a new field of two-dimensional nanostructures, first comprising freestanding graphene,<sup>1</sup> followed by boron nitride,<sup>2</sup> and transition metal dichalcogenide (TMD)<sup>3</sup> graphene-like nanosheets, created clear possibilities for implementing many new nanomaterials in science, technology and industry. In contrast to the monolayers of graphene or *h*-BN, monolayers of MoS<sub>2</sub> and WS<sub>2</sub> consist of three-atom thick slabs in which each metal atom is sandwiched between two layers of chalcogen atoms.

WS<sub>2</sub> and MoS<sub>2</sub> nanosheets have peculiar electronic properties (a semiconducting band gap and high mobility of the carriers) which allow one to potentially apply these nanomaterials in the fields of nanoelectronics and nanophotonics.<sup>3</sup> The potential for application of 2D TMDs in nanoelectronics can be further strengthened by cutting them into nanoribbons. This leads to a drastic change in the electronic, mechanical, and optical properties of these materials. There has been a number of theoretical papers showing that MoS<sub>2</sub> (ref. 4 and 5) and WS<sub>2</sub> (ref. 6) nanoribbons display semiconducting or metallic

properties depending on their width and type of edges. Nowadays ultra-narrow MoS<sub>2</sub> and WS<sub>2</sub> nanoribbons can be fabricated inside and outside of carbon nanotubes.<sup>5–7</sup> Also, MoS<sub>2</sub> nanorods and nanoflakes have been fabricated.<sup>8,9</sup> However, until recently, there have been no reports regarding the fabrication of freestanding TMD nanoribbons.

It is well known that graphene nanoribbons can be fabricated through unzipping of carbon nanotubes by various methods.<sup>10,11</sup> TMDs can also form tubular structures similar to carbon nanotubes,<sup>12</sup> which can also be potentially unzipped into ribbons and nanoflakes, which has recently been shown for the case of WS<sub>2</sub>.<sup>13,14</sup> This work may establish a universal approach for nanotube unzipping and nanoribbon synthesis. Unpacking of the WS<sub>2</sub> nanotubes (WS<sub>2</sub>NTs) was caused by the lithiation and further intercalation by organic 1-octanethiol molecules followed by sonication. Therefore the underlining hypothesis of the current work was the following: the interaction between the 1-octanethiol molecules and lithium ions led to the penetration of the 1-octanethiol molecules between the nanotube layers, especially between the outer layers, which caused the elastic expansion of the outer layers of the nanotube. Therefore, herein we focus on the theoretical verification of the process of WS<sub>2</sub>NT unzipping. We based our work on the experimental fact that the unzipping of WS<sub>2</sub>NTs is caused by the intercalation of lithiated nanotubes with organic molecules (1-octanethiol). We then address a hypothesis that penetration of the 1-octanethiol molecules between the nanotube walls leads to the radial expansion and further disruption of the nanotube followed by unzipping of the whole nanotube. The strain energy of the expanded tubes was calculated using continuum thin-

<sup>a</sup>National University of Science and Technology MISiS, 4 Leninskiy prospekt, Moscow, 119049, Russian Federation. E-mail: dgkvashnin@gmail.com

<sup>b</sup>Emanuel Institute of Biochemical Physics of RAS, 119334 Moscow, Russian Federation  
<sup>c</sup>Technological Institute of Superhard and Novel Carbon Materials, 7a Centralnaya Street, Troitsk, Moscow, 142190, Russian Federation

<sup>d</sup>Moscow Institute of Physics and Technology, 9 Institutskiy lane, Dolgoprudny, 141700, Russian Federation

<sup>e</sup>Department of Materials and Interfaces, Weizmann Institute, Rehovot 76100, Israel

<sup>f</sup>World Premier International (WPI) Center for Materials Nanoarchitectonics, (MANA), National Institute for Materials Science (NIMS), Namiki 1-1, Tsukuba, Ibaraki 3050044, Japan

walled cylinder approximation in the first part of the paper. Using the computed parameters for the WS<sub>2</sub> lattice, the dependence of the deformation energy of the tubes upon the circumferential strain was then obtained. In the second part of the paper, we studied the intercalation of lithiated WS<sub>2</sub>NTs by a reference organic molecule (1-octanethiol) and estimated the energy gain of this process, which can be used for expanding the layers and eventually unzipping the tube. The comparison of the energy gain with the elastic strain allows us to estimate the dependence of the diameter of the WS<sub>2</sub>NTs upon the concentration of the embedded 1-octanethiol molecules. The third part of the paper is devoted to the computational validation of the fact that, by densely packing organic molecules, a strained WS<sub>2</sub>NT can be unzipped into a nanoribbon. In the final part, the electronic structures of the initial WS<sub>2</sub>NT and resulting WS<sub>2</sub> nanoribbon were discussed and compared with available theoretical and experimental data.<sup>13</sup>

## Results and discussion

Fig. 1a and b show representative transmission electron microscopy (TEM) and high-resolution TEM (HRTEM) images of the starting WS<sub>2</sub> nanotubes. Fig. 1c and d depict the initial and final stages of the nanotube unzipping, as detailed in ref. 13.

It is now important to theoretically understand and verify the process behind the unzipping of the WS<sub>2</sub>NTs; this description is the main point of the present work. The working hypothesis of the present study, as judged from previously conducted experiments, is related to the elastic expansion of the intercalated

tube. Subsequent sonication of the structure leads to the unzipping of already highly strained WS<sub>2</sub>NTs.

It was assumed that the continuum structure equivalent to WS<sub>2</sub>NT is an isotropic thin-walled cylinder with the mean diameter of the corresponding nanotube. The elastic expansion of the tube causes hoop stress,  $\sigma_h$ , which reduces the tube length and induces longitudinal stress  $\sigma_L$  (radial stress is neglected). Therefore, we can describe the strain of the tube by Hooke's law as follows:<sup>15,16</sup>

$$\varepsilon_h = \frac{\sigma_h}{Y} - \frac{\nu\sigma_L}{Y} = \frac{PR}{2Yh}(2 - \nu); \quad \sigma_h = \frac{PR}{h}; \quad \sigma_L = \frac{PR}{2h}, \quad (1)$$

where,  $\varepsilon_h$  is the hoop strain,  $Y$  and  $\nu$  are the in-plane Young's modulus and Poisson ratio of the continuum structure equivalent, respectively,  $P$  is the internal pressure which causes the expansion and  $R$  is the radius of the tube. Due to ambiguity in the single WS<sub>2</sub> layer thickness determination we used the in-

plane stiffness equation  $C = Yh = \frac{1}{A_0} \frac{\partial^2 U}{\partial \varepsilon^2}$  (where  $U$  is the strain energy computed per unit cell,  $A_0$  is the equilibrium surface area of a WS<sub>2</sub> sheet and  $\varepsilon$  is the uniaxial strain). Therefore, the final expression for the strain energy,  $U$ , of the expanded continuum structure in terms of in-plane stiffness and hoop strain can be expressed by the following:

$$U = \frac{2C\varepsilon_h^2}{2 - \nu} S = \frac{2C\varepsilon_h^2}{2 - \nu} 2\pi Rl, \quad (2)$$

where  $S$  is the area of a WS<sub>2</sub> nanotube unit cell,  $l$  is the cell parameter in the axial direction. Values for the in-plane stiffness and Poisson ratio can be obtained directly from the *ab initio* calculations, and were defined as 237.04 N m<sup>-1</sup> and 0.3, respectively.

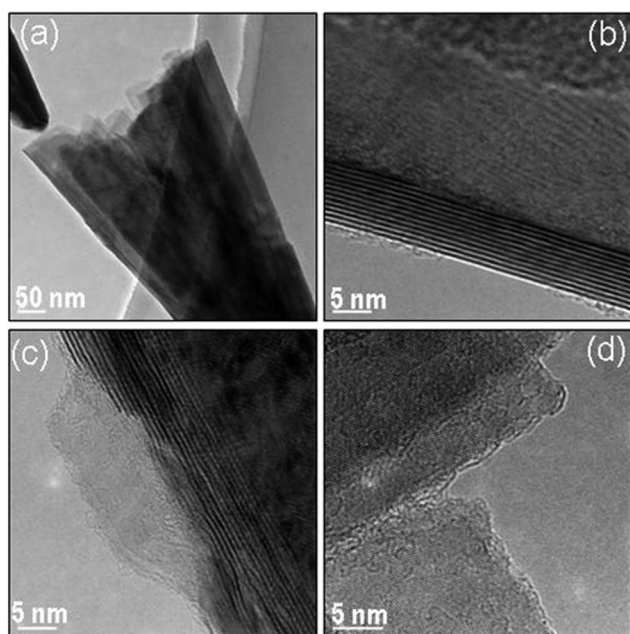


Fig. 1 (a) Low-magnification TEM image of a WS<sub>2</sub> nanotube bundle; (b) high-resolution TEM image of a nanotube wall showing multi-layers; (c and d) HRTEM images of partially and fully unzipped nanotubes revealing atomically-resolved images of the WS<sub>2</sub> nanoribbons.

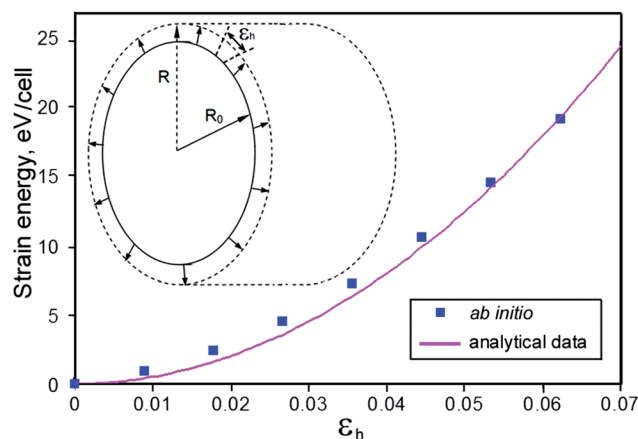


Fig. 2 Strain energy of a (9,9) WS<sub>2</sub> nanotube as a function of the hoop strain for analytical data (solid curve) and *ab initio* calculations (points). The inset illustrates a schematic representation of the initial and the strained nanotube.

In Fig. 2, a comparison between the *ab initio* calculations and isotropic cylindrical tube approximation is shown for the case of a (9,9) WS<sub>2</sub> nanotube (similar results were obtained for tubes with different diameters and chirality). The close agreement

between the two data sets validates the chosen continuum model. This data is used for the evaluation of the strain within the elastically deformed WS<sub>2</sub> nanotubes intercalated by lithium ions and 1-octanethiol molecules.

In the next step, we considered the penetration mechanism of the 1-octanethiol molecules between the WS<sub>2</sub>NT walls based on the assumption that the attractive driving force of the 1-octanethiol molecule is its interaction with the intercalated Li ions. *Ab initio* calculations show that the 1-octanethiol molecule binds to a lithium atom with an energy gain of  $-0.29$  eV. If instead of a neutral atom the charged ion Li<sup>+</sup> (due to the charge transfer to the nanotube walls) is considered, the energy gain rises to  $-1.35$  eV.

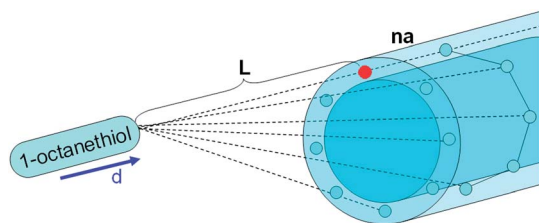


Fig. 3 Schematic model of the interaction between the dipole,  $d$ , of the 1-octanethiol molecule and the set of a point charges representing the Li<sup>+</sup> ions. The closest Li ion to the 1-octanethiol molecule is marked in red.

In addition, non-chemical interactions between the large dipole of 1-octanethiol and an array of positive point charges representing Li<sup>+</sup> ions were taken into account. The calculations show that the 1-octanethiol molecule has a dipole moment of  $2.9$  D. It was assumed that each 1-octanethiol molecule interacts with all of the lithium ions arranged between the nanotube walls uniformly (Fig. 3) with the exception of the first lithium ion located before the 1-octanethiol molecule (marked as the red ball in Fig. 3). The contribution of this first Li<sup>+</sup> was already taken into account during the *ab initio* calculation of the chemical reaction energy. It was suggested that Li<sup>+</sup> ions are densely packed between the walls without chemically binding with each other. Indeed, the distance between the neighboring intercalated Li<sup>+</sup> is about  $4$  Å, which is larger than the crystalline Li–Li bond length ( $2.67$  Å) and larger than the distance in the molecular ion Li<sub>2</sub><sup>+</sup> ( $3.14$  Å).

The energy of the electrostatic interaction between the dipole and the set of point charges is defined as:

$$E_{\text{dip}} = qE|\vec{L} + n\vec{a}| = \frac{1}{4\pi\epsilon\epsilon_0} \frac{qd}{R^3} |\vec{L} + n\vec{a}| \sqrt{1 + 3\cos^2(\theta)},$$

$$n = 0 \dots \infty, \quad (3)$$

where  $d$  is an absolute value of the dipole moment of the 1-octanethiol molecule;  $q$  is the charge of the lithium ion;  $R = |\vec{L} + n\vec{a}|$  is the distance between the 1-octanethiol molecule and a given point charge;  $L$  is the distance between the dipole and the closest Li<sup>+</sup> from the first ring of a point charges ( $2.5$  Å);  $\theta$  is the angle between the dipole direction and the point charge;  $\epsilon$  is the relative permittivity of the 1-octanethiol solvent (in which

WS<sub>2</sub> nanotubes were unzipped in the original experiment<sup>13</sup>) which equals  $3.896$  F m<sup>-1</sup>.<sup>17</sup> Based on these estimates we can conclude that the value of the energy released during the interaction between the dipole (1-octanethiol molecule) and the set of point charges equals  $0.19$  eV and the total energy gain from the interaction of the 1-octanethiol molecule with the lithium ions is  $1.35 + 0.19 = 1.54$  eV per 1-octanethiol molecule.

Assuming that all of the gained energy is used for the radial expansion of the tube, the comparison between the strain energy due to expansion and released energy due to the interaction of 1-octanethiol with the Li<sup>+</sup> ions allows us to obtain a diagram of the dependence of the strain energy on the hoop strain of the tubes of different radii, see Fig. 4. This diagram offers a visual estimation of the degree of nanotube stretching at a given concentration of penetrated molecules.

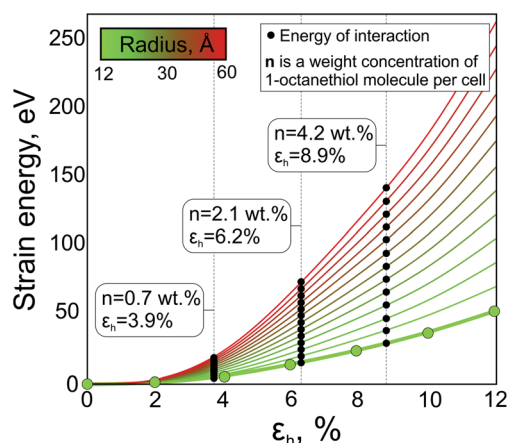


Fig. 4 Dependence of the calculated strain energy upon the hoop strain,  $\epsilon_h$ , for WS<sub>2</sub> nanotubes of different radii (from 12 to 60 Å). The black dots are the values of the total energy of interaction between the 1-octanethiol molecule and the lithium ions at various 1-octanethiol weight concentrations,  $n$ , the intercalation of which causes the nanotube expansion with the corresponding hoop strain,  $\epsilon_h$ . The radius of the unstretched WS<sub>2</sub> nanotube is marked by the color gradient (from green,  $R = 12$  Å, to red,  $R = 60$  Å). The results of the DFT calculation for the WS<sub>2</sub> nanotube (16,16) ( $R = 12$  Å) are depicted by green circles.

From Fig. 4 it can be concluded that the energy released from the reaction between the 1-octanethiol molecules and the lithium ions with the maximum possible concentration (every C<sub>8</sub>H<sub>18</sub>S molecule is paired with every Li<sup>+</sup> ion and occupies five WS<sub>2</sub> unit cells,  $n = 4.2$  wt%) is high enough to stretch the WS<sub>2</sub> nanotube by up to 8.9%. We subsequently carried out an *ab initio* molecular dynamics (MD) simulation to understand if this concentration is sufficiently large for the unzipping of the nanotube wall. Due to limited computational resources, it is only possible to simulate a small double-walled nanotube (9,9) @ (16,16). Moreover, due to the same limitation, it is not possible to use 1-octanethiol molecules in this simulation, therefore CH<sub>4</sub> molecules, with nearly the same molecular lateral size, were considered. The concentration of CH<sub>4</sub> molecules was taken to be 9 molecules per unit cell, which corresponds to

$n = 2.1$  wt%, as depicted in Fig. 4. The relaxation of the nanotube with intercalated  $\text{CH}_4$  molecules leads to the expansion of the tube by 7.6%, which corresponds to the obtained analytical data (6.2%) and verifies our estimations.

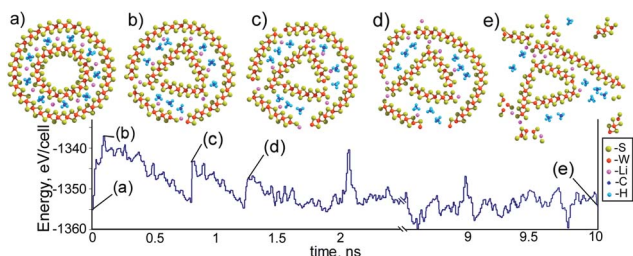


Fig. 5 Potential energy and structural changes of a (9,9)@(16,16) intercalated  $\text{WS}_2$  nanotube in MD simulations at  $T = 1000$  K during a 10 ns period. The insets show the crucial moments in the structure evolution: (a) the initial structure of (9,9)@(16,16)  $\text{WS}_2$  nanotube with intercalated lithium atoms and methane molecules; (b) first detachment of the part of the outer nanotube wall; (c) detachment of the next part of the nanotube wall; (d) partial deformation of the inner nanotube wall and (e) a final unzipped structure obtained from the (9,9)@(16,16) nanotube with a resulting zigzag nanoribbon  $12\text{ZWS}_2\text{NR}$ .

The molecular dynamics simulation was carried out with a time step of 1 fs, and the total simulation period was 10 ns. The most significant stages in the MD simulation period are shown in Fig. 5 together with the corresponding energy profile of the system. The temperature of the simulation was taken as 1000 K because it is not possible to simulate the long relaxation process at ambient temperatures. The double-walled nanotube without intercalated Li ions and  $\text{CH}_4$  molecules is stable, whereas the results of the MD evolution show (Fig. 5) that the intercalated structure was unzipped and a zigzag  $\text{WS}_2$  nanoribbon with index 12 (according to the classification of graphene nanoribbons,  $12\text{ZWS}_2\text{NR}$ ) was formed. To validate the nanotube unzipping mechanism, in addition, a metadynamics simulation at 300 K of the same (9,9)@(16,16)  $\text{WS}_2\text{NT}$  was carried out. The simulation showed that the unzipping process had taken place after 800 metasteps at 300 K. This fact allows us to conclude that the mechanism leading to  $\text{WS}_2$  nanotube unzipping is correct.

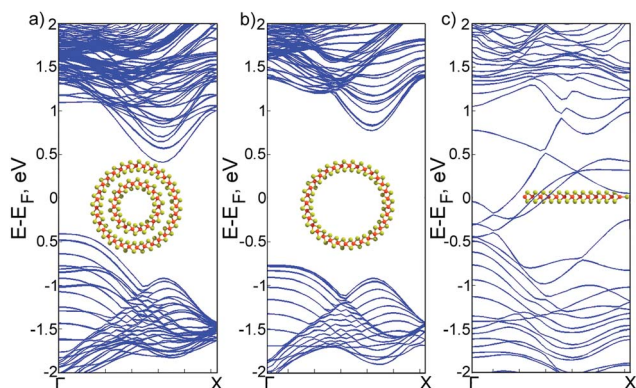


Fig. 6 Band structure of (a) (9,9)@(16,16)  $\text{WS}_2\text{NT}$ ; (b) (16,16)  $\text{WS}_2\text{NT}$  and (c)  $12\text{ZWS}_2\text{NR}$ . The Fermi level energy is taken as zero.

We also investigated the electronic properties of an initial double-walled  $\text{WS}_2$  nanotube (9,9)@(16,16), a single-walled  $\text{WS}_2$  nanotube (16,16) and the nanoribbon obtained from the unzipping of the former nanotube. In Fig. 6 the band structures of the considered objects are presented. As one can see, both double- and single-walled  $\text{WS}_2$  nanotubes display semiconducting properties with indirect band gaps of 0.9 eV and 1.55 eV, respectively, while the formed nanoribbon displays a metallic character. This finding is in good agreement with the previously published papers<sup>6</sup> and the latest work<sup>13</sup> which is the prime focus of the present study.

## Conclusion

A simple model describing the latest experimental data of the unzipping process of  $\text{WS}_2$  nanotubes<sup>13</sup> is presented. Based on the experimental fact that the effect of unzipping is caused by the intercalation of lithiated multi-walled  $\text{WS}_2\text{NTs}$  by 1-octanethiol molecules, the hypothesis that the main reason for unzipping is the expansion of nanotube walls is proposed. The salient features of the penetration mechanism of the molecules between the nanotube walls are presented. It is found that the approach and binding of the 1-octanethiol molecules with the nanotube-intercalated  $\text{Li}^+$  ions is energetically favourable. The mechanical deformation of the nanotube walls is described using continuum thin-walled cylinder approximation with parameters evaluated from *ab initio* calculations. It is shown that using values of the in-plane stiffness ( $C$ ) of  $237.04 \text{ N m}^{-1}$  and a Poisson ratio ( $\nu$ ) of 0.3 provides an excellent agreement between the analytical and the DFT-calculated data. Comparing the energy gain due to the interaction of the 1-octanethiol molecule with  $\text{Li}^+$  and the energy loss due to the elastic expansion of the wall, it is found that the penetration of 1-octanethiol between the nanotube walls can stretch a  $\text{WS}_2$  nanotube by up to 8.9% at a concentration of 4.2 wt% of 1-octanethiol molecules. In order to understand if this strain is sufficiently large to lead to the nanotube wall unzipping, a molecular dynamics simulation at 1000 K and a metadynamics simulation at 300 K of a small double-walled (9,9)@(16,16)  $\text{WS}_2$  nanotube system were carried out (in the simulation a smaller concentration corresponding to 2.1 wt% of 1-octanethiol molecules was used). It is demonstrated that even under these circumstances the (9,9)@(16,16)  $\text{WS}_2$  nanotube unzips and forms a  $\text{WS}_2$  nanoribbon with index 12 ( $12\text{ZWS}_2\text{NR}$ ). The investigated nano-objects display different types of conductivity. It was finally concluded that the process of unzipping allows the fabrication of metallic planar  $\text{WS}_2$  nanoribbons from semiconducting tubes. The present results support recent experimental data and can pave the way toward the fabrication of transition metal dichalcogenide nanostructures with various electronic properties.

## Methods

### Computational details

Our calculations were performed using density functional theory<sup>18,19</sup> within the generalized gradient approximation of

the Perdew–Burke–Ernzerhof<sup>20</sup> parameterization with periodic boundary conditions using the Vienna *Ab initio* Simulation Package.<sup>21–23</sup> PAW along with a plane wave basis set with an energy cutoff of 300 eV was used. To calculate the atomic and electronic structures, the Brillouin zone was sampled according to the Monkhorst–Pack<sup>24</sup> scheme with 8 and 32 *k*-points in a periodical direction. To avoid spurious interactions between neighboring structures in a tetragonal supercell, a vacuum layer of 15 Å in all nonperiodic directions was included. Structural relaxation was performed until the forces acting on each atom became less than 0.05 eV Å<sup>-1</sup>. The unit cell of the investigated double-walled WS<sub>2</sub>NT, with intercalated lithium atoms and methane molecules, included up to 300 atoms depending on the NT radius. The molecular dynamics simulations were carried out at a constant temperature using the Nosé–Hoover thermostat.<sup>25,26</sup> The temperature was taken as 1000 K. The total time of simulation was 10 ns with the time step 1 fs. The atomic structure was written after every ionic step. Metadynamics calculations were performed under conditions of an Andersen thermostat<sup>27</sup> at a constant temperature of 300 K. The idea of metadynamics is the introduction of a history-dependent potential term, which fills the minima in the free energy surface. In this way the system can not go back to previously visited states until it could cross the energy barriers and undergo phase transitions.<sup>28</sup> History-dependent potential was constructed as a sum of Gaussians centered along the trajectory of the collective variables. Updating of bias potential by addition of Gaussian functions was made after each ionic step. The height of a Gaussian hill was taken as 10<sup>-3</sup> eV and the Gaussian width was taken as 10<sup>-3</sup> in units of the collective variables.

## Acknowledgements

This work was supported by the Ministry of Education and Science of the Russian Federation (Agreement No. 11.G34.31.0061) within the Mega-Grant Program for the leading scientists (D.G.). We are grateful to the ‘Chebishev’ and ‘Lomonosov’ supercomputers of Moscow State University and the Joint Supercomputer Center of the Russian Academy of Sciences for the possibility of using a cluster computer for our quantum-chemical calculations. P.B.S., D.G.K. and L.Yu.A. acknowledge the support by the Russian Scientific Fund (Contract No. 14-13-01217). D.G.K. also acknowledges the support from the Russian Ministry of Education and Science (Contract No. 948 from 21 November 2012). R.T. acknowledges the support of the EU- ERC INTIF 226639 and EU-ITN Project MoWSeS 317451 projects. The authors are grateful to A.G. Kvashnin, Drs. C. Nethravathu, N. Kawamoto and Prof. Y. Bando for useful discussions.

## References

- 1 K. S. Novoselov, *Rev. Mod. Phys.*, 2011, **83**, 837.
- 2 D. Golberg, Y. Bando, Y. Huang, T. Terao, M. Mitome, C. Tang and C. Zhi, *ACS Nano*, 2010, **4**, 2979.
- 3 Q. H. Wang, K. Kalantar-Zadeh, A. Kis, J. N. Coleman and M. S. Strano, *Nat. Nanotechnol.*, 2012, **7**, 699.
- 4 Y. F. Li, Z. Zhou, S. B. Zhang and Z. F. Chen, *J. Am. Chem. Soc.*, 2008, **130**, 16739.
- 5 Z. Wang, H. Li, Z. Liu, Z. Shi, J. Lu, K. Suenaga, S. K. Joung, T. Okazaki, Z. Gu, J. Zhou, *et al.*, *J. Am. Chem. Soc.*, 2010, **132**, 13840.
- 6 Z. Wang, K. Zhao, H. Li, Z. Liu, Z. Shi, J. Lu, K. Suenaga, S. Joung, T. Okazaki, Z. Jin, *et al.*, *J. Mater. Chem.*, 2011, **21**, 171.
- 7 Z. Liu, K. Suenaga, Z. Wang, Z. Shi, E. Okunishi and S. Iijima, *Nat. Commun.*, 2011, **2**, 213.
- 8 B. Visic, R. Dominko, M. K. Gunde, N. Hauptman, S. D. Skapin and M. Remskar, *Nanoscale Res. Lett.*, 2011, **6**, 593.
- 9 X. Zheng, L. Zhu, A. Yan, C. Bai and Y. Xie, *Ultrason. Sonochem.*, 2004, **11**, 83.
- 10 J. K. Dustin and J. M. Tour, *Macromol. Chem. Phys.*, 2012, **213**, 1033.
- 11 L. Ma, J. Wang and F. Ding, *ChemPhysChem*, 2013, **14**, 47.
- 12 R. Tenne, L. Margulis, M. Genut and G. Hodes, *Nature*, 1992, **360**, 444.
- 13 C. Nethravathi, A. A. Jeffery, M. Rajamathi, N. Kawamoto, R. Tenne, D. Golberg and Y. Bando, *ACS Nano*, 2013, **7**, 7311.
- 14 C. L. Choi, J. Feng, Y. Li, J. Wu, A. Zak, R. Tenne and H. Dai, *Nano Res.*, 2013, **6**, 921.
- 15 R. T. Fenner, *Mechanics of Solids*, Blackwell Sci. Pub., Oxford, London, Edinburgh, Boston, Melbourne, 1989.
- 16 J. M. Gere and S. P. Timoshenko, *Mechanics of Materials*, PWS Pub. Co., Boston, 1997.
- 17 V. K. Agarwal, A. K. Sharma and P. Kumar, *J. Chem. Eng. Data*, 1977, **22**, 127.
- 18 P. Hohenberg and W. Kohn, *Phys. Rev.*, 1964, **136**, B864.
- 19 W. Kohn and L. J. Sham, *Phys. Rev.*, 1965, **140**, A1133.
- 20 J. P. Perdew, K. Burke and M. Ernzerhof, *Phys. Rev. Lett.*, 1996, **77**, 3865.
- 21 G. Kresse and J. Hafner, *Phys. Rev. B: Condens. Matter*, 1993, **47**, 558.
- 22 G. Kresse and J. Hafner, *Phys. Rev. B*, 1994, **49**, 14251.
- 23 G. Kresse and J. Furthmüller, *Phys. Rev. B*, 1996, **54**, 11169.
- 24 H. J. Monkhorst and J. D. Pack, *Phys. Rev. B*, 1976, **13**, 5188.
- 25 W. G. Hoover, *Phys. Rev. A: At., Mol., Opt. Phys.*, 1985, **31**, 1695.
- 26 S. Nosé, *J. Chem. Phys.*, 1984, **81**, 511.
- 27 H. C. Andersen, *J. Chem. Phys.*, 1980, **72**, 2384.
- 28 A. Laio and M. Parrinello, *Proc. Natl. Acad. Sci. U. S. A.*, 2002, **99**, 12562.